MEASUREMENTS OF THE TRAVEL TIME OF SHEAR WAVES IN GRANULAR SOILS USING BENDER ELEMENTS

Mesures de temps de parcours des ondes de cisaillement dans des chantillons de sols granulaires à l'aide de capteurs de type "bender elements"

Juan AYALA[1], Felipe VILLALOBOS[1], Alejandro ALEJO[2]
[1] *Laboratory of GeoMaterials, Catholic University of Concepción, Concepción, Chile*
jlayala@ing.ucsc.cl, avillalobos@ucsc.cl
[2] *Department of Electrical Engineering, Catholic University of Concepción, Concepción, Chile*
aalejo@ucsc.cl

ABSTRACT - The shear wave velocity is becoming a commonly used parameter by Geotechnical Engineers for determining G_0. This work describes the measurement of the travel time of shear waves in a soil sample, where bender elements are set up in an oedometer apparatus. Experiments were carried out for different relative densities, saturation states, types of transmitted waves, frequencies as well as wave amplitudes, changes in the diameter of the soil sample and load state. Different criteria for evaluating the arrival times of shear waves to the receiving element, both in time domain and in the frequency domain are studied. Besides some repeatability statistics were assessed.

1. Introduction

Since 2011 it has become a compulsory norm to measure shear wave velocities V_s for medium to major building projects in Chile. This paper describes an especially constructed set up to measure V_s in the laboratory. To achieve that travel times are actually measured and analyzed for different conditions. The soil maximum shear modulus defined by elasticity as $G_0 = \rho V_s^2$, is calculated by V_s and by the density of the soil material ρ. Finally, travel time recognition is assessed by different methods.

2. Apparatus description

An oedometer apparatus was adapted to put a sand sample in a specially built box. Two cylindrical boxes for soil samples of 44.8 and 70.2 mm inside diameter, and a maximum travel length of 56 mm from bender elements tip to tip were used. See Ayala (2013) for details of the equipment set up.

3. Differences of the time arrival

Measurements of travel times for single sine pulse (in most of the cases tested) for different frequencies, sample diameters, relative densities, loading and moisture states are presented. Additionally, the differences between the arrival time for different shape pulses are showed.

The stacking algorithm of the oscilloscope allows the removal of significant noise by averaging 128 received signals, where the triggered pulses have 10 or 20 ms between them.

3.1. Frequency and loading

The travel times shown in Figure 1 belong to the same sand sample of 44.8 mm diameter for loading states from 25 to 400 kPa and for different frequencies from 1 to 15 kHz of the driver signal.

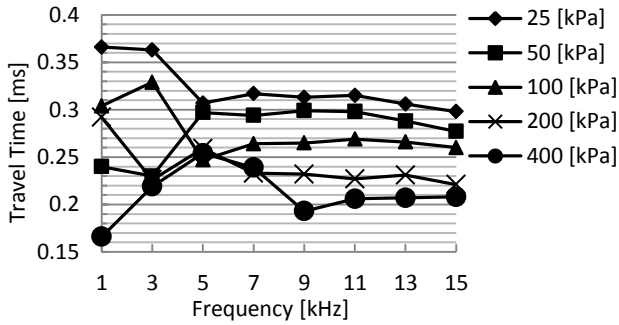

Figure 1 Travel times for relative density RD = 85%

A delay time of 10 minutes was waited between different loading states, so there's no more axial deformation between loading states. Settlements lesser than 0.01 mm were observed, which were included in the distance tip to tip.

Moreover, in Figure 1 it can be noted that for frequencies below 9 kHz the arrival times does not follow a regular value. This is because there is not enough tip to tip distance between the sensors for these low frequencies of the driver signal. For instance, if a value of V_s = 250 m/s = 250 mm/ms is assumed for the tip to tip distance of 55 mm, the driver frequency *f* needed to have at least one wave length between the bender's tip is *f* = 250 mm/ms/55 mm = 4.5 1/ms = 4.5 kHz. Yamashita *et*

al. (2009) recommend having at least 2 wave lengths in the oedometer apparatus to avoid the near field effect NFE. So for 2 wave lengths f = 2·4.5 kHz = 9 kHz, just when the data start to show regularity, not only in Figure 1, but also in the following data acquired in this investigation.

It is also worth observing in Figure 1 that when the load is incremented the travel time decreases. This is because of the decreasing in the distance tip to tip between the bender elements and de increasing of the relative density of the soil.

3.2. Frequency and sample diameter

For both sample diameters irregular travel times were found for frequencies below 9 kHz as shown in Figure 2. Figure 2 shows the travel times for 400 kPa and sand samples with DR = 85%.

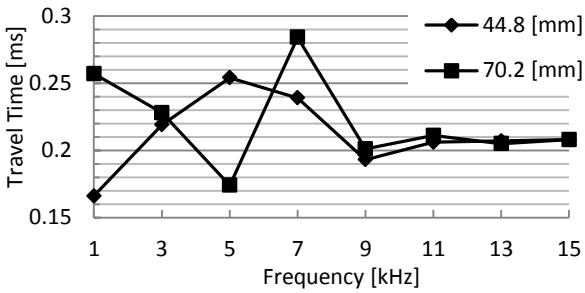

Figure 2 Difference between diameters

The main problem for the travel times below 9 kHz is due to the difficulty in choosing the first wave arrival. Waves are clearly shown in some frequencies, but some of them disappear in other frequencies. However, appearance and disappearance of waves in the received signal stops at 9 kHz and above.

Figure 2 shows clearly that for this two sample diameters and for 9 to 15 kHz there is not important difference in travel times. Furthermore, this indicates the range of frequencies for which V_s and G_0 should be sought in the tests.

3.3. Frequency in saturated sample

Travel times showed before correspond to dry samples. Dense saturated sand samples with DR = 85% were tested under a pressure of 400 kPa.

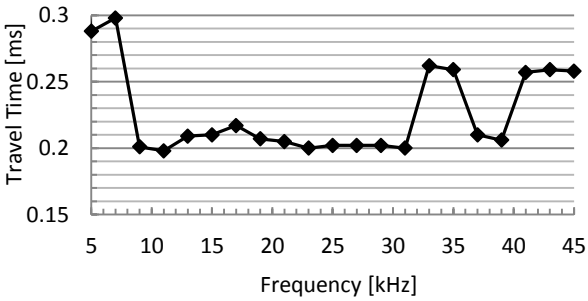

Figure 3 Saturated sample at 400 kPa

Figure 3 shows that the travel time in the saturated sample becomes also regular for a frequency of around 9 kHz. The main difference is the shape of the received signal wave. It has an important component probably from compression waves and cross talk that does not let to find clearly the arrival of the shear wave.

But also for frequencies above 9 kHz there are clearly separated waves in the signal which facilitate the determination of the travel time with any frequency between 9 and 31 kHz. Abode 31 kHz the decreased signal makes hard to find the first arrival time.

3.4. Frequency and shape wave

When the received signals were analysed it was hard to define the first arrival wave for the lower frequencies signals. When the data was collected, the horizontal (time) scale of the oscilloscope remain the same and the time differences for the lower frequencies between the start and the first maximum of the driver signal were too big for the travel time of the distance tip to tip pre-defined.

As discussed before, to have at least one wave length as distance between the bender elements, 4.5 kHz has to be used, but to avoid any trouble, at least 2 wave length is recommended, i.e. 9 kHz. Another aspect considered is the wave shape. Figure 4 shows three wave shapes applied to the sand sample. It can be observed that for square waves travel times are more regular than for the ramp and sine waves in the frequency range tested.

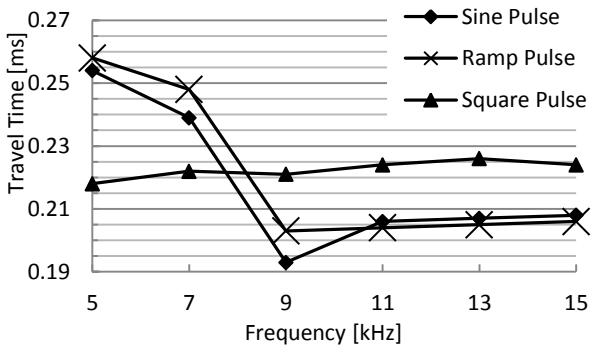

Figure 4 Different wave shapes

For the driving pulses with sine and ramp shape, the arrival times were impossible to determine for frequencies between 1 and 3 kHz, for that reason they are omitted. Nevertheless, for the range from 5 to 15 kHz they tend to have the same arrival time with variation smaller than 0.05 ms. On the other hand the square shape pulse maintains almost the same travel time with an average of 0.22 ms indifferent from the frequency of the driving pulse.

3.5. Loading and saturation

Figure 5 shows the travel time curves for different loading states (25, 50, 100, 200 and 400 kPa), frequencies (11 and 15 kHz) and saturation.

It can be seen in Figure 5 that for 25 kPa the differences in travel time between the saturated and dry samples are bigger than for larger loading states. In addition, there is a small reduction in travel time for the higher frequency as also shown in Figure 1.

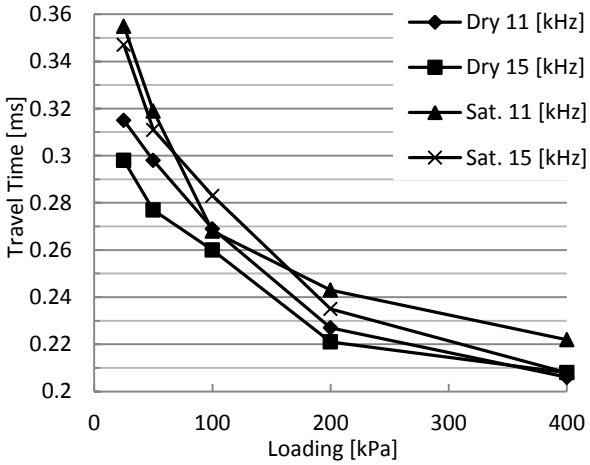

Figure 5 Loading and saturation

It is clear to notice that the travel time decreases when the loading increases. Comparing the same test for dry and saturated samples (11 kHz, 200 kPa and 85% RD), the travel time is 0.227 and 0.222 ms, respectively. The travel time decrease in 0.005 ms because of saturation is not significant.

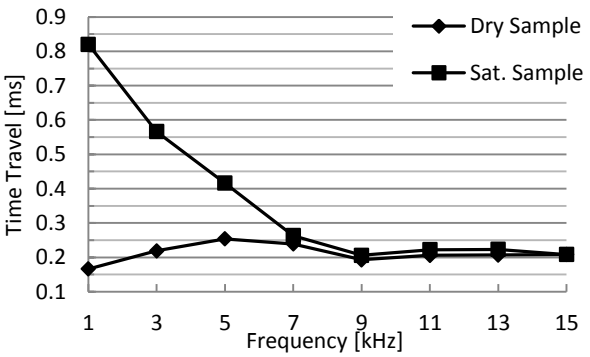

Figure 6 Frequency and saturation for 400 kPa

Figure 6 shows the relation between travel times for different frequencies and saturation. Again for frequencies adobe 9 kHz the travel time is regular and almost the same. For the saturated sample the travel time is slightly higher than for dry samples.

3.6. Loading and relative density RD

Figure 7 shows a decrease in the travel time for the increase of dry sand RD as well as with loading pressure (as already shown in Figure 5). This has direct implications in V_s and G_0, i.e. they increase with RD and loading pressure.

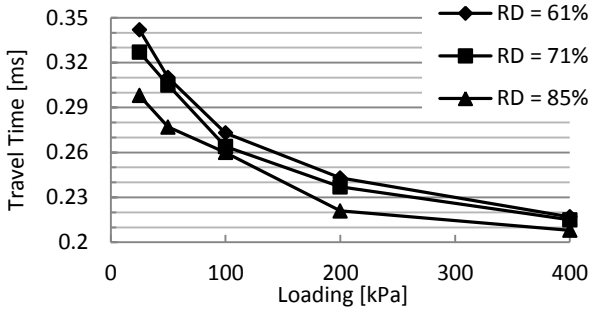

Figure 7 Different RD and loading pressures

3.7. Time and frequency domain techniques

Two curves of travel times in Figure 8 have been determined using the Cross Correlation method. With this method the time "t_{cc}" correspond to the maximum value obtained. The value of t_{cc} corresponds to the time shift as described by Viggiani and Atkinson (1995).

The other two curves "t_d" correspond to the time domain selection of the arrival shear wave.

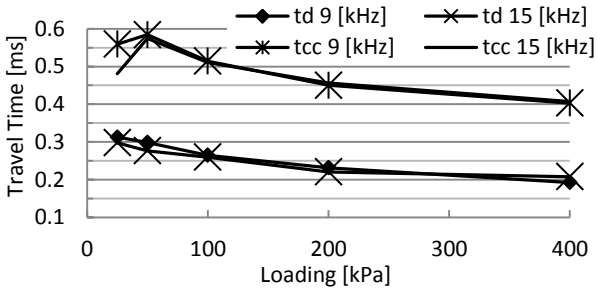

Figure 8 Time arrivals for two different methods

The main difference between these two methods is that Cross Correlation analysis assumes that the travel time is equal to the time shift t_{cc}. In the time domain analysis t_d corresponds to the first wave which does not have necessarily the larger amplitude.

4. Differences of the received signal voltage

The influence of the driving signal amplitude is very important because it is directly related to the driving bender element deformation. This affects the received signal amplitude. A high attenuation of the received signal will insinuate that the driving signal should work with a higher voltage, within the limits of the bender element and the electric system used.

4.1. Frequency and driver signal voltage

The following test results were obtained for loading pressures of 400 kPa and with dry samples. In Figure 9, the gain for different driven frequencies and different driven amplitudes from 5 to 20 V peak

to peak (V_{p-p}), are shown. The gain is defined as the ratio between the amplitude of the received signal and the triggered signal. It can be observed in Figure 9 that for higher frequencies the gain is larger than for small frequencies. This occurs because for higher frequencies the received wave amplitude is larger than for small frequencies.

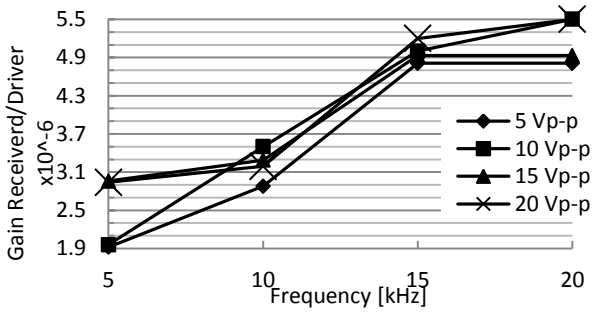

Figure 9 Gain Ratio for dry samples and 400 kPa

4.2. Relation between driver and received signal voltages

The plot of voltages peak to peak V_{p-p} for the received and triggered signal is shown in Figure 10. It can be indicated that for higher driver signal voltages, higher voltages of the received signal are obtained. In addition, for higher frequencies and for the same driver amplitude, higher voltages in the received signal were obtained.

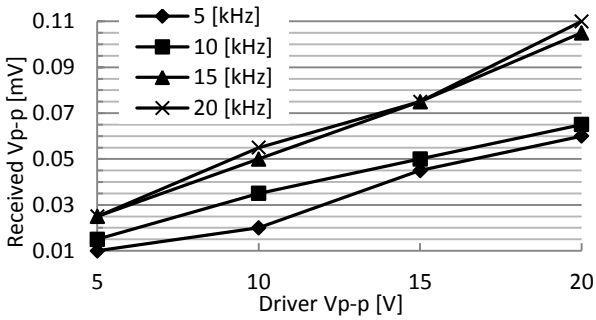

Figure 10 Received and driver V_{p-p} signals

5. Repeatability statistics

To verify the repeatability of results, 51 and 50 tests were repeated using 56% RD dry samples in 44.8 and 70.2 mm diameter, respectively. The plot of the 51 received signals for the smaller diameter sample and 20 V_{p-p} trigger, 10 kHz are shown in Figure 11. In dashed line is shown the triggered signal.

The software R of the Foundation for Statistical Computing was used to evaluate the probability distribution of the travel times from Figure 11. For this, the non-parametric test of Kolmogorov-Smirnov was used. The result of the statistical test was that there is not enough evidence to deny the hypothesis that the data of the 51 travel times has a normal distribution. In the Figure 12 it is shown the histogram for the the data that has a mean value of 0.243 ms.

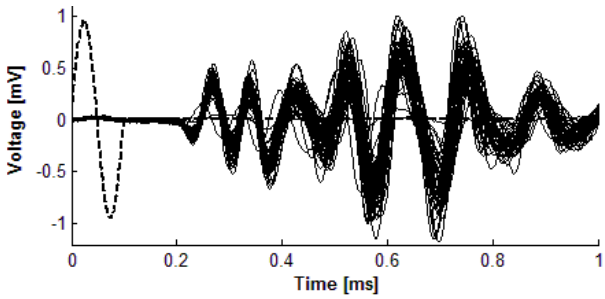

Figure 11 51 Received signals

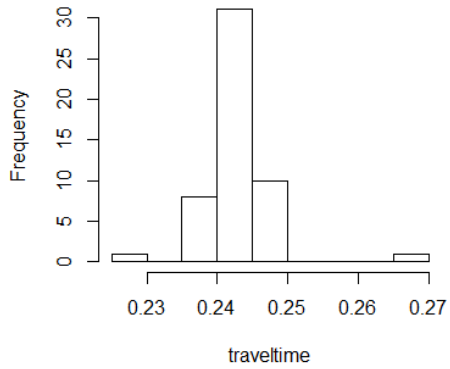

Figure 12 Histogram of the 51 travel times

6. Conclusions

No big differences were found in the variations of sample diameter or saturation state over the 9 kHz driver signal. As was expected a lower travel time were found for higher loading states and relative densities. The square signal it is more conservative. The input frequency it is more significant than the driver voltage to have a bigger gain at the same loading state. A linear relation was found between driver and received signals voltages. It was proven that the test is repeatable. It is recommended to make an input frequency mapping for each different sample, loading and saturation state, in order to have a better received signal to analyze.

7. References

Ayala, J.L. (2013). Experimental study of shear waves propagation in granular soils using bender elements in the oedometric equipment. M.Sc. thesis, UCSC

Viggiani, G., and Atkinson, J. H. (1995). Interpretation of bender elements tests. *Géotechnique 45*, 149-154.

Yamashita, S., Kawaguchi, T., Nakata, Y., Mikami, T., Fujiwara, T., and Shibuya, S. (2009). Interpretation of international parallel test on the measurements of Gmax using bender elements. *Soils and Foundations Vol. 49*, 631-650.